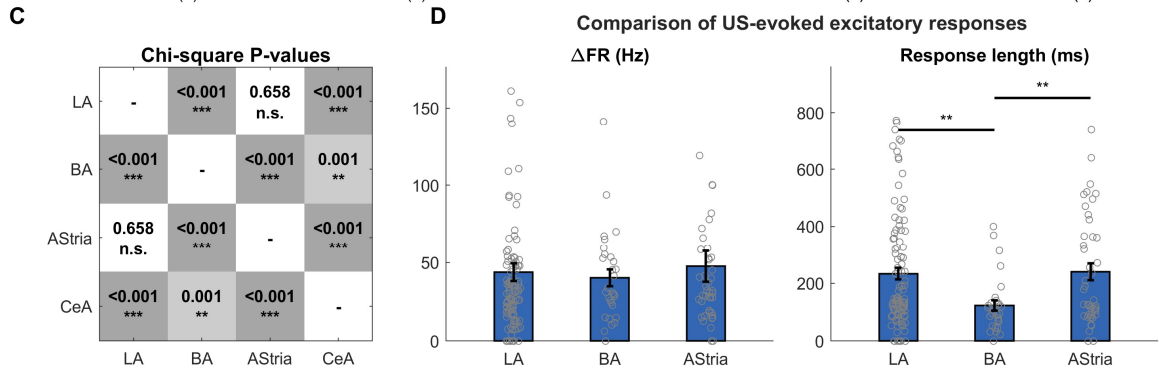
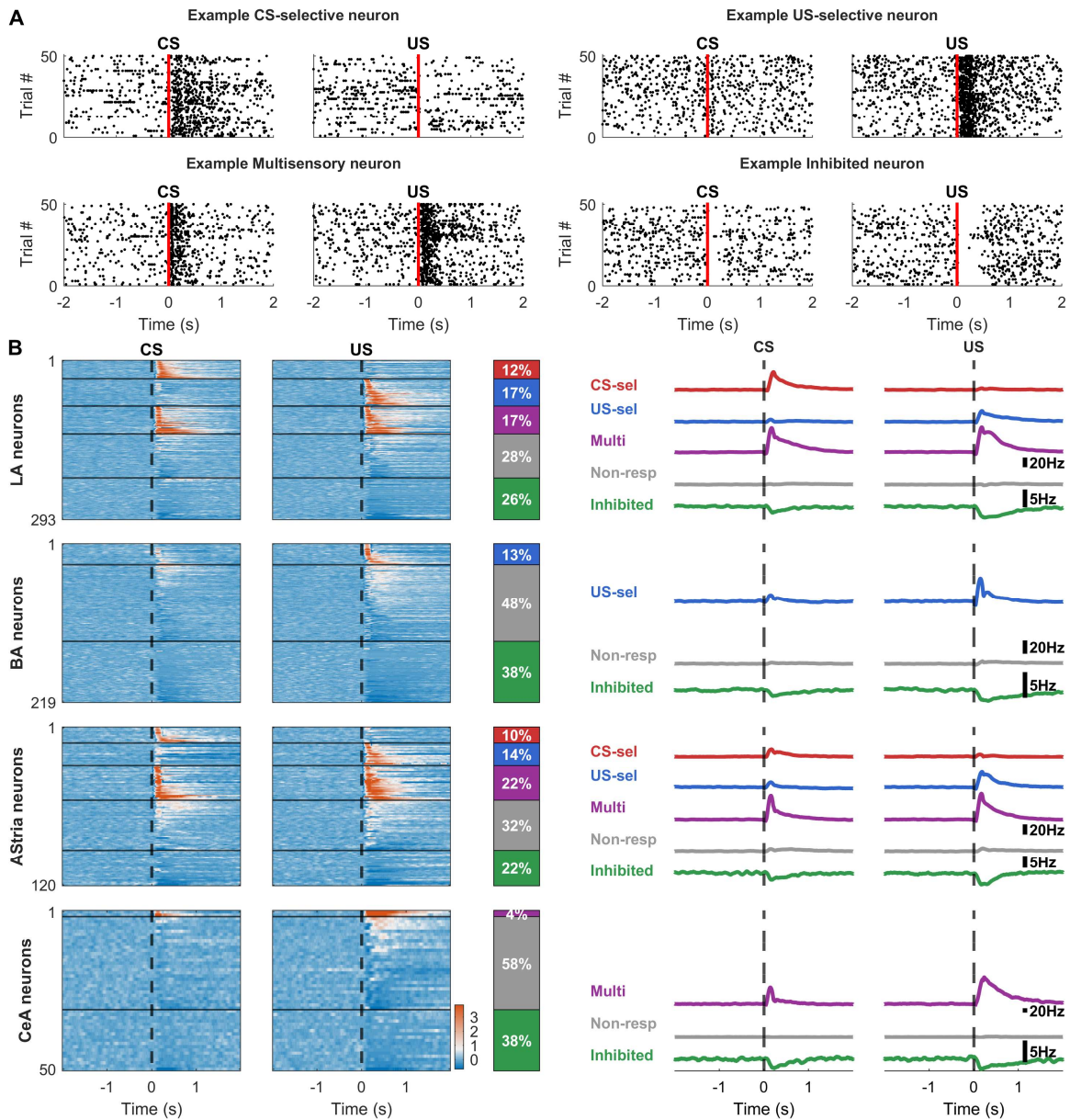


**Figure 1: Characterization of neurons in the basal amygdala during fear conditioning**

**(A)** Experimental setup schematic showing mouse with headplate implantation, auditory conditioned stimulus (CS; 3 kHz, 50 ms tone), and unconditioned stimulus (US; 10 ms tail-shock). **(B)** Example neuronal responses to CS (left) and US (right). Top: raw voltage traces showing single-trial responses. Red signs indicate the stimulus types, dashed lines the stimulus onset (time 0), and gray shading shows the US-evoked artefact duration removed before analysis. **(C)** Example interspike interval (ISI) distributions for putative principal neurons (PN, left, blue) and fast spiking interneurons with narrow spike width (IN, right, magenta). Insets show autocorrelograms (ACG, top) with 20 ms scale bar, and

average waveforms (bottom) with 0.5 ms scale bar. **(D)** Spike feature classification. Left: scatter plot of trough-to-peak time versus firing rate for LA and BA neurons. Dashed lines indicate classification boundaries (0.4 ms and 10 Hz). Right: normalized waveforms (z-score) for PNs (blue, n=472) and INs (magenta, n=40), showing mean  $\pm$  SD. **(E)** Firing rate distributions across brain regions (LA, BA, Astria, CeA). LA and BA show separate distributions for PNs (blue) and INs (magenta). Astria and CeA show combined distributions (gray). Log-spaced bins from 0.1 to 30 Hz. **(F)** Burst index distributions (Royer et al., 2012) across brain regions. Same color scheme as panel E. Log-spaced bins from 0.1 to 100.



**Figure 2: Regional differences in neuronal response profiles to fear conditioning stimuli.**

**(A)** Example single-neuron raster plots for CS (left) and US (right) stimuli. Top to bottom: CS-selective neuron, US-selective neuron, Multisensory neuron, and inhibited neuron. Red vertical lines mark stimulus onset. **(B)** Population responses across four brain regions (LA, BA, AStria, CeA). Columns 1-2: Z-scored heatmaps for CS and US trials, sorted by stimulus preference. Column 3: Bar charts showing cluster proportions (CS-selective: red, US-selective: blue, Multisensory: purple, Non-responsive: gray, Inhibited: green). Columns 4-5: Average firing rate (Hz) for CS and US trials, showing mean response for each cluster with Savitzky-Golay smoothing (201 bins). **(C)** Chi-square test p-value matrix comparing cluster distributions across regions. Grayscale intensity indicates significance level: darker gray for  $p < 0.001$ , lighter gray for  $p < 0.05$ , white for  $p \geq 0.05$ . Text shows exact p-values and significance markers ( $***p < 0.001$ ,  $**p < 0.01$ ,  $*p < 0.05$ ). Note the similarity between neuronal spiking in the LA and AStria. **(D)** Comparison of US-evoked excitatory response metrics across LA, BA, and AStria. Three bar graphs show the difference in firing rate ( $\Delta FR$ , Hz) and response length (ms) for US-selective and Multisensory neurons combined. Individual data points shown as circles; bars represent mean  $\pm$  SEM. Statistical comparisons use Kruskal-Wallis test with post-hoc pairwise Mann-Whitney U tests.

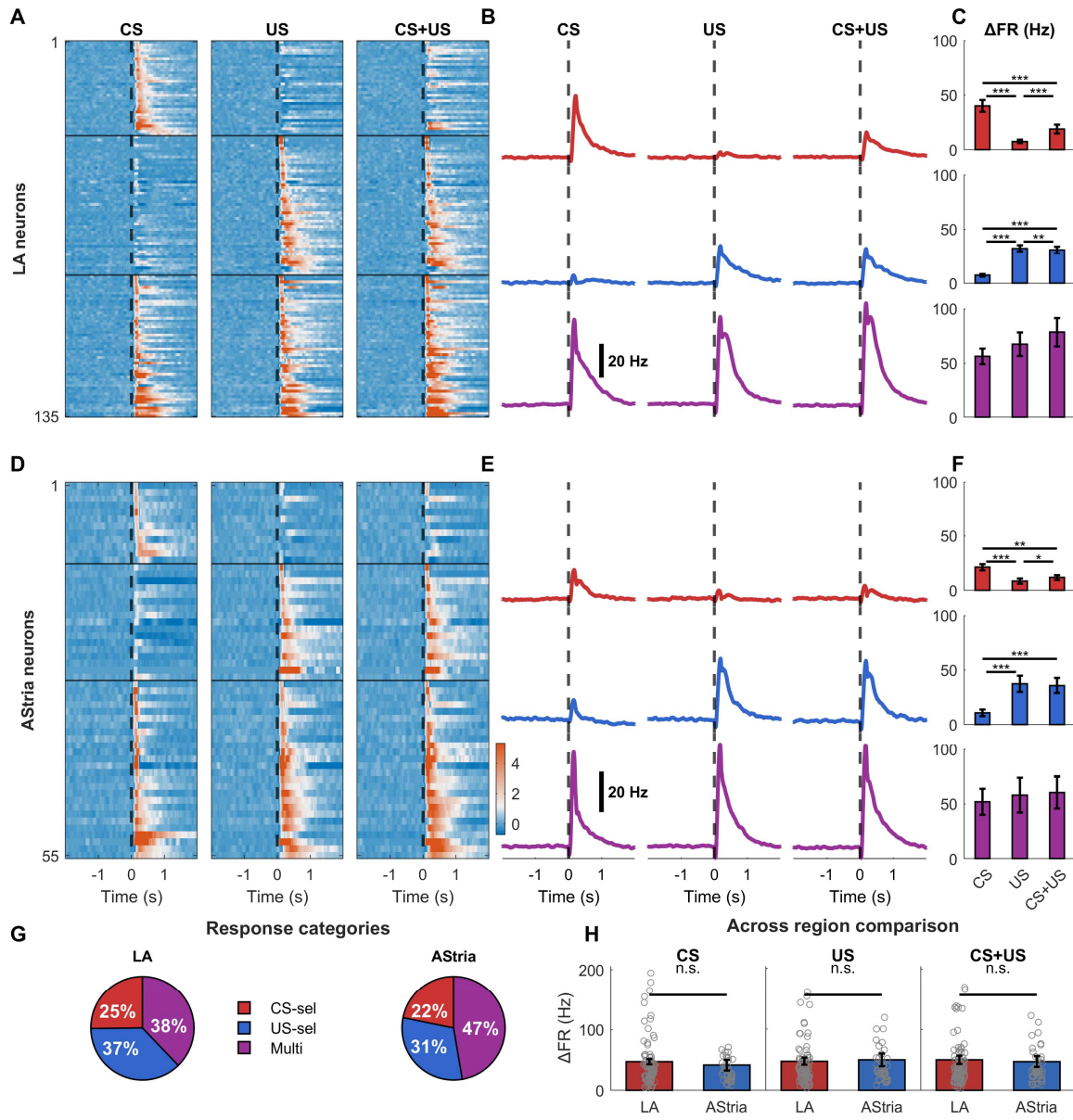


**Figure 3: Similar properties of CS-selective, US-selective, and Multisensory neurons in the LA and AStria.**

(A) LA heatmaps showing z-scored PSTHs for CS (left), US (middle), and CS+US (right) stimuli. Neurons sorted by cluster (CS-selective, US-selective, Multisensory, non-responsive, inhibited) based on CS and US responses only. Color scale shows z-score normalized to baseline. Black lines separate clusters. (B) Lines showing population average firing rates (Hz) for CS-selective (red), US-selective (blue), and Multisensory (purple) neurons. Each cluster displayed separately (stacked rows) for CS, US, and CS+US stimuli. Scale bar: 20 Hz. (C) LA bar charts showing delta firing rate ( $\Delta FR$ ) comparing CS, US, and CS+US responses within each cluster. Bars show mean  $\pm$  SEM. Statistical comparisons use Wilcoxon signed-rank test (\* $p<0.05$ , \*\* $p<0.01$ , \*\*\* $p<0.001$ ). (D) AStria heatmaps, same format as panel A. (E) Lines, same format as panel B. (F)

AStria bar charts, same format as panel C. **(G)** Similar proportions of CS-selective, US-selective, and Multisensory neurons in LA (left) and AStria (right). Percentages indicate fraction of responsive neurons in each category. Legend shows cluster color coding. **(H)** Delta peak firing rate ( $\Delta$ FR) for CS (left), US (middle), and CS+US (right) responsive neurons in the LA and AStria is similar. Individual data points shown as grey circles with jitter. Bars show mean  $\pm$  SEM. Statistical comparison using Wilcoxon rank-sum test (\* $p<0.05$ , \*\* $p<0.01$ , \*\*\* $p<0.001$ , n.s.=not significant). Y-axis scaled to 95th percentile to avoid compression from outliers.

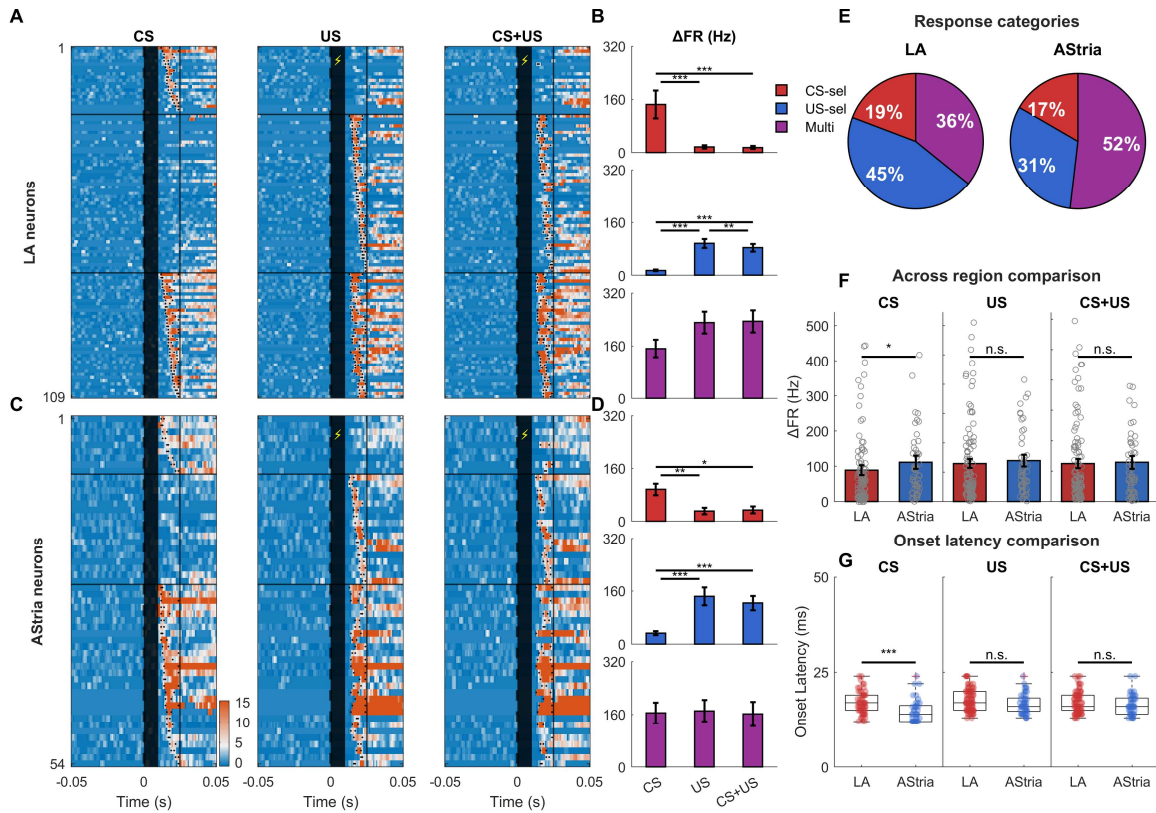


**Figure 4: Monosynaptic responses to fear conditioning stimuli are similar in the LA and AStria.**

**(A)** Heatmaps of monosynaptic responses in the LA showing z-scored PSTHs for CS (left), US (middle), and CS+US (right) stimuli. Only neurons with detected responses in the monosynaptic window (0-25ms post-stimulus) are shown, sorted by cluster (CS-selective, US-selective, Multisensory). Color scale shows z-score normalized to baseline. Black lines separate clusters. **(B)** Delta peak firing rate ( $\Delta$ FR, Hz) bar charts comparing CS, US, and CS+US responses for each LA cluster. Stacked vertically: CS-selective (top), US-selective (middle), Multisensory (bottom). Bars show mean  $\pm$  SEM. Statistical comparisons use Wilcoxon signed-rank test (\* $p<0.05$ , \*\* $p<0.01$ , \*\*\* $p<0.001$ ). **(C)** Heatmaps of monosynaptic responses in the AStria, same format as panel A. **(D)** AStria delta peak firing rate (Hz) bar charts, same format as panel B. **(E)** Pie charts showing similar proportions of CS-selective, US-selective, and Multisensory neurons among monosynaptic responders in the LA (left) and AStria (right). Percentages indicate fraction of monosynaptic neurons in each category. **(F)** Across region comparison of delta peak firing rate ( $\Delta$ FR, Hz) for CS (left), US (middle), and CS+US (right) monosynaptic responders comparing LA vs AStria neurons. Individual data points shown as grey circles with jitter. Bars show mean  $\pm$  SEM. Statistical comparison using Wilcoxon rank-sum test (\* $p<0.05$ , \*\* $p<0.01$ , \*\*\* $p<0.001$ , n.s.=not significant). Y-axis scaled to 95th percentile to avoid compression from outliers. **(G)** Onset latency comparison for monosynaptic responses. Three panels show CS, US, and CS+US onset latencies (ms)

comparing LA vs AStria neurons. Bars show mean  $\pm$  SEM. Statistical comparison using Wilcoxon rank-sum test (\* $p<0.05$ , \*\* $p<0.01$ , \*\*\* $p<0.001$ , n.s.=not significant).

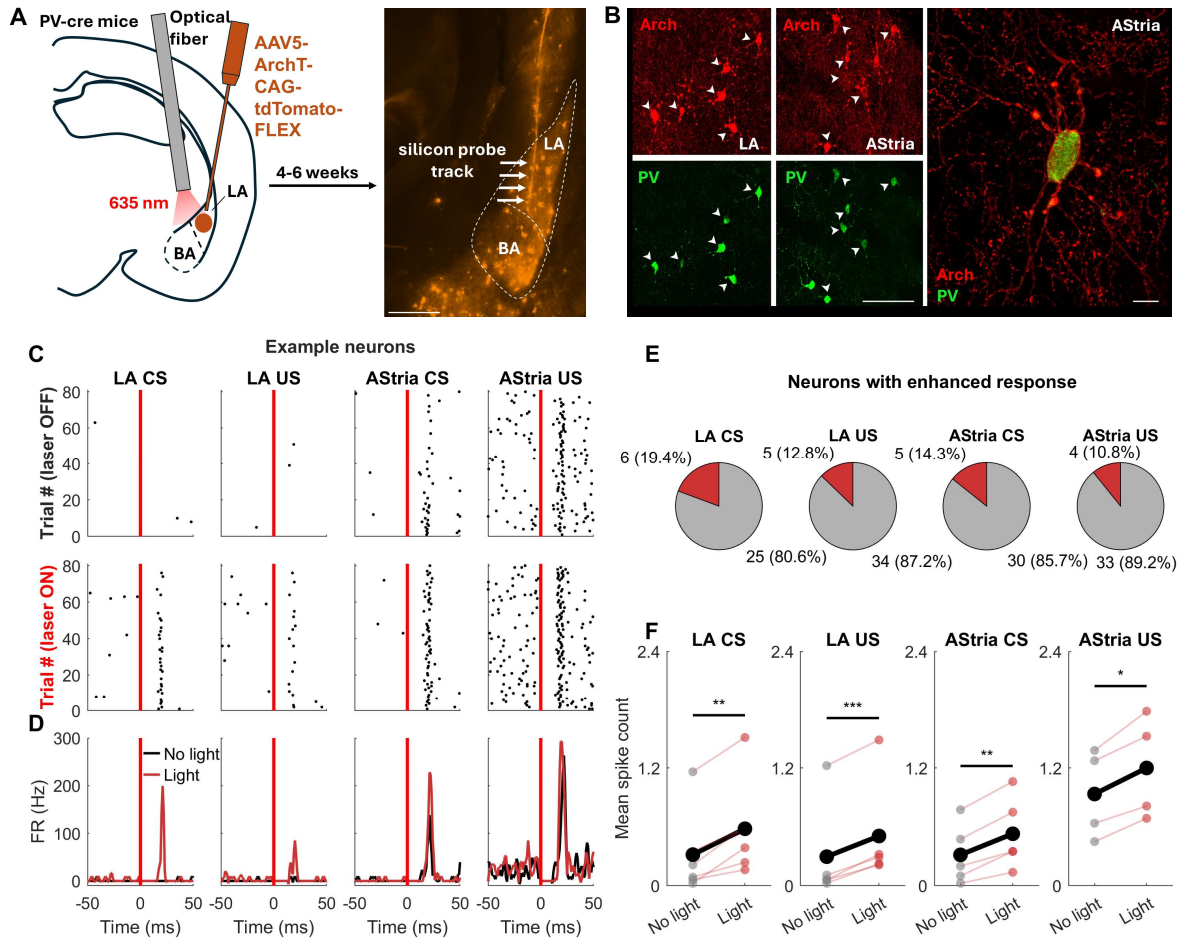
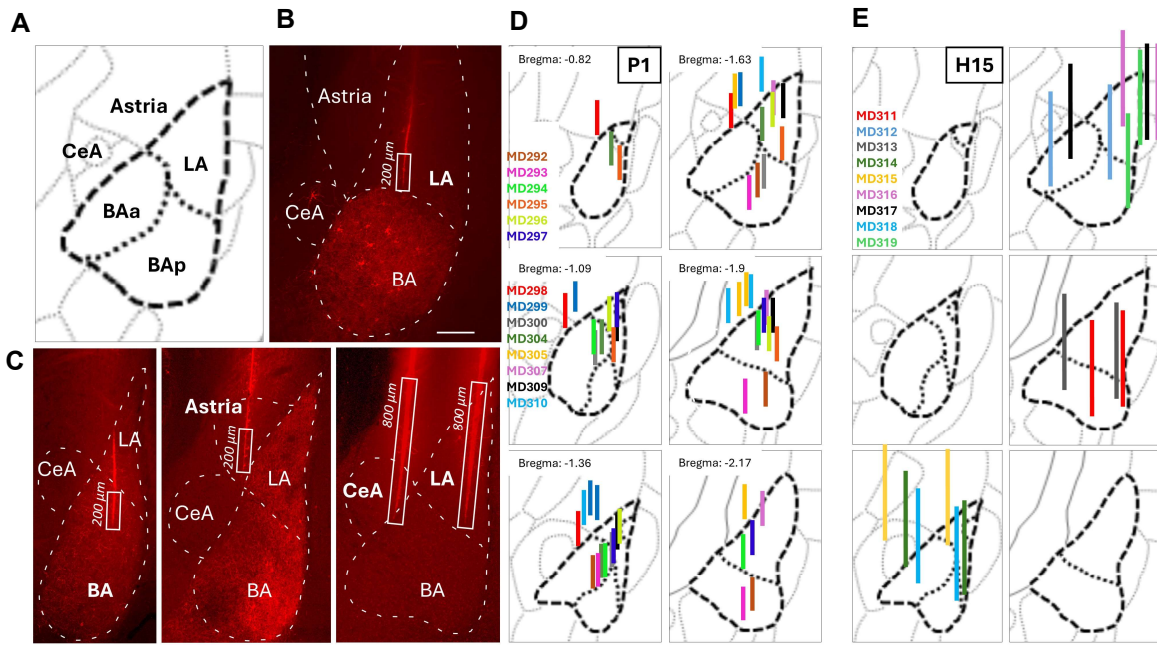


**Figure 5: A fraction of monosynaptic responses in the LA and AStria are controlled by PV interneurons.**

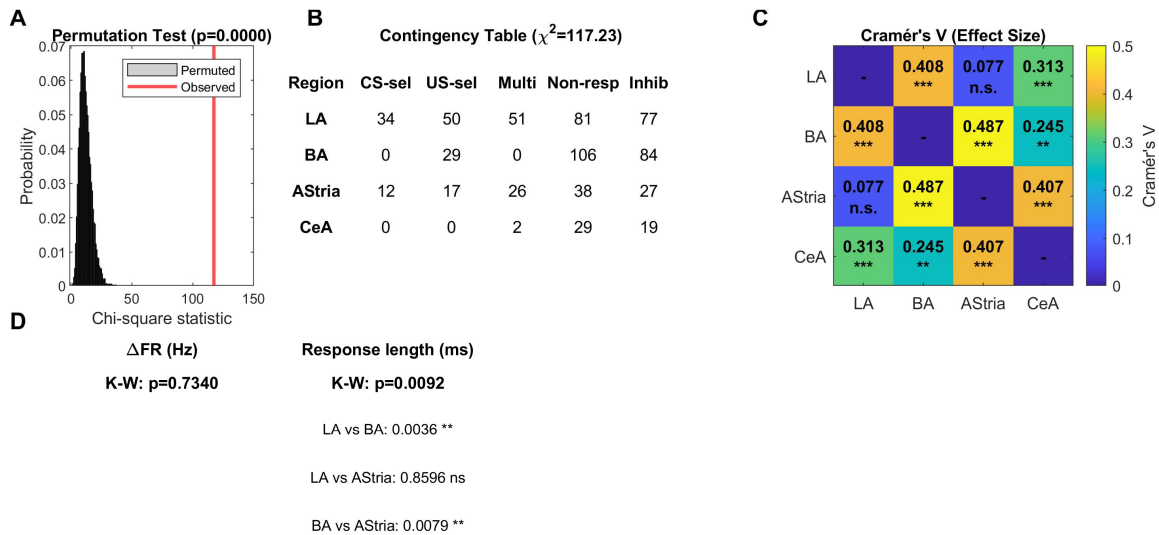
**(A)** Left: Schematic of stereotaxic injections in PV-Cre mice. AAV5-ArchT-CAG-tdTomato-FLEX virus was delivered into the LA and AStria, followed by implantation of an optical fiber positioned above the LA for 635-nm light delivery to inhibit PV-expressing interneurons. Following 4–6 weeks of viral expression, a silicon probe was inserted to record neural activity during optogenetic manipulation. Right: Representative fluorescence image showing tdTomato-expressing neurons in the BA and LA, along with the track of the silicon probe (arrows). Dashed lines outline the anatomical boundaries of the LA and BA. **(B)** Left: Micrographs showing Arch-expression (top) in PV-positive neurons (bottom) in the LA and AStria. Right: Individual, PV-positive AStria neuron expresses Arch throughout the membrane. Scale bars: left, 100  $\mu$ m; right, 10  $\mu$ m. **(C)** Example raster plots showing individual neuron responses to CS or US stimuli without light (top row) and with light (middle row) for four example neurons. Each row represents one trial, with spike times shown as vertical marks. Red vertical line indicates stimulus onset. **(D)** Lines for the same example neurons showing average firing rate (Hz) over time for no-light (black) and light (red) conditions. Time axis centered at stimulus onset (0 ms). Each plot shows the peristimulus time histogram comparing baseline and

optogenetic manipulation conditions. **(E)** Pie charts showing proportions of neurons with enhanced (red) vs non-enhanced (gray) monosynaptic responses during inhibiting PV interneurons. Numbers and percentages indicate fraction of responsive neurons in each category. **(F)** Plots showing trial-averaged spike counts for individual enhanced neurons comparing no-light (left, black) vs light (right, red) conditions. Each gray line represents one neuron, with population mean shown in bold. Four panels correspond to LA CS, LA US, AStria CS, and AStria US enhanced neurons. Enhancement detected using Wilcoxon signed-rank test ( $p<0.05$ ) comparing spike counts in the monosynaptic window (12-50 ms) between light and no-light conditions.



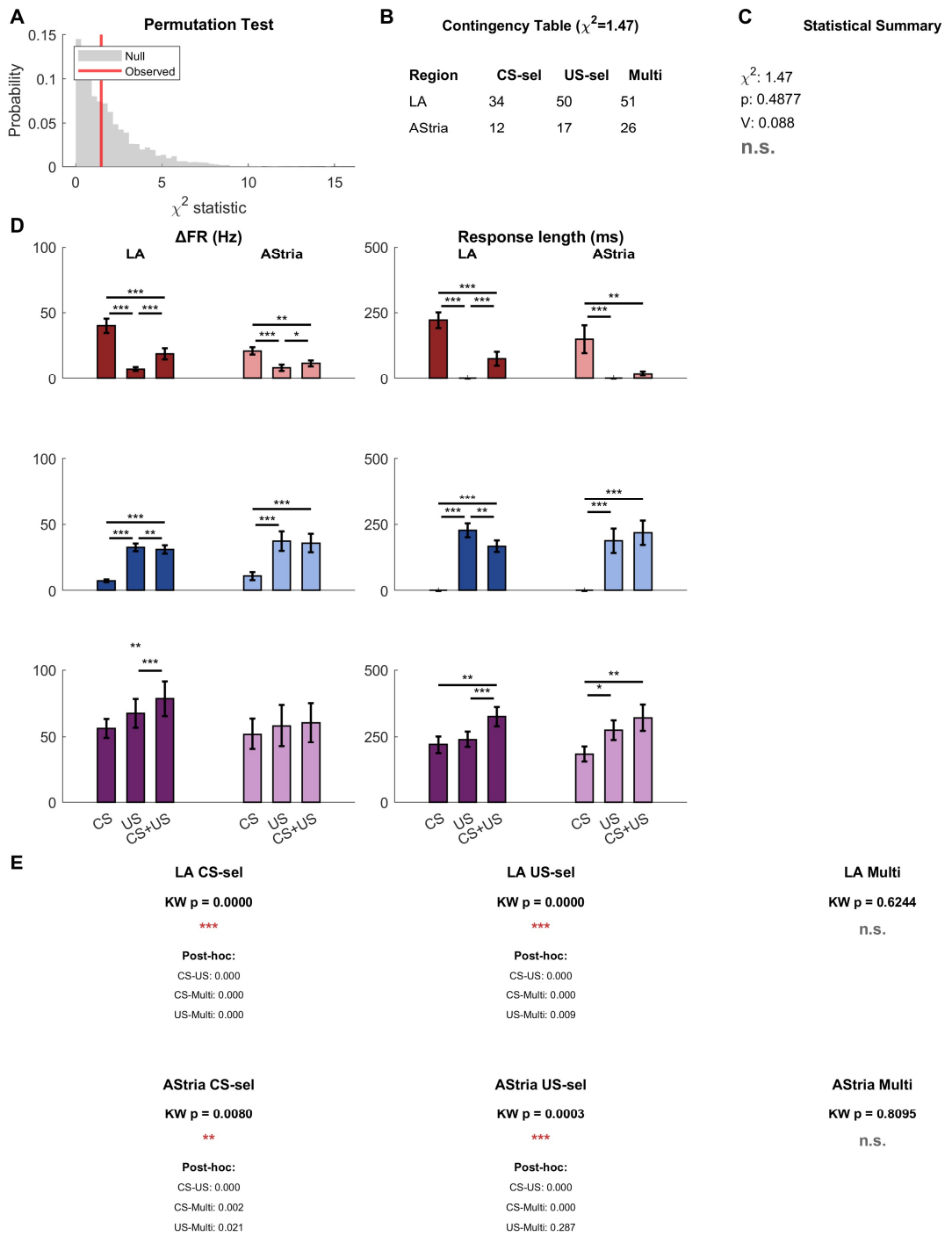
### Supplementary Figure 1: Position of electrode tracks in the BLA, CeA and Astria.

**(A)** Schematic map of the BLA, CeA and Astria. **(B)** Recording electrode tracks in LA. White boxes indicate the distribution of recording sites in inhibitory opsin (Archeorhodopsin) -injected tissue. **(C)** Example images of recording sites in BA/LA (left), Astria (middle) and CeA/LA (right) recordings. **(D)** Schematics present the distribution of recording electrodes in different experiments (each color represents a distinct animal) using the P1 probe (4 shanks, 200 µm of recording sites on tip). **(E)** as in (D) using the H15 probe (2 shanks, 800 µm of recording sites on tip). Scale: 200 µm



### Supplementary Figure 2: Statistical analysis of cluster distribution differences

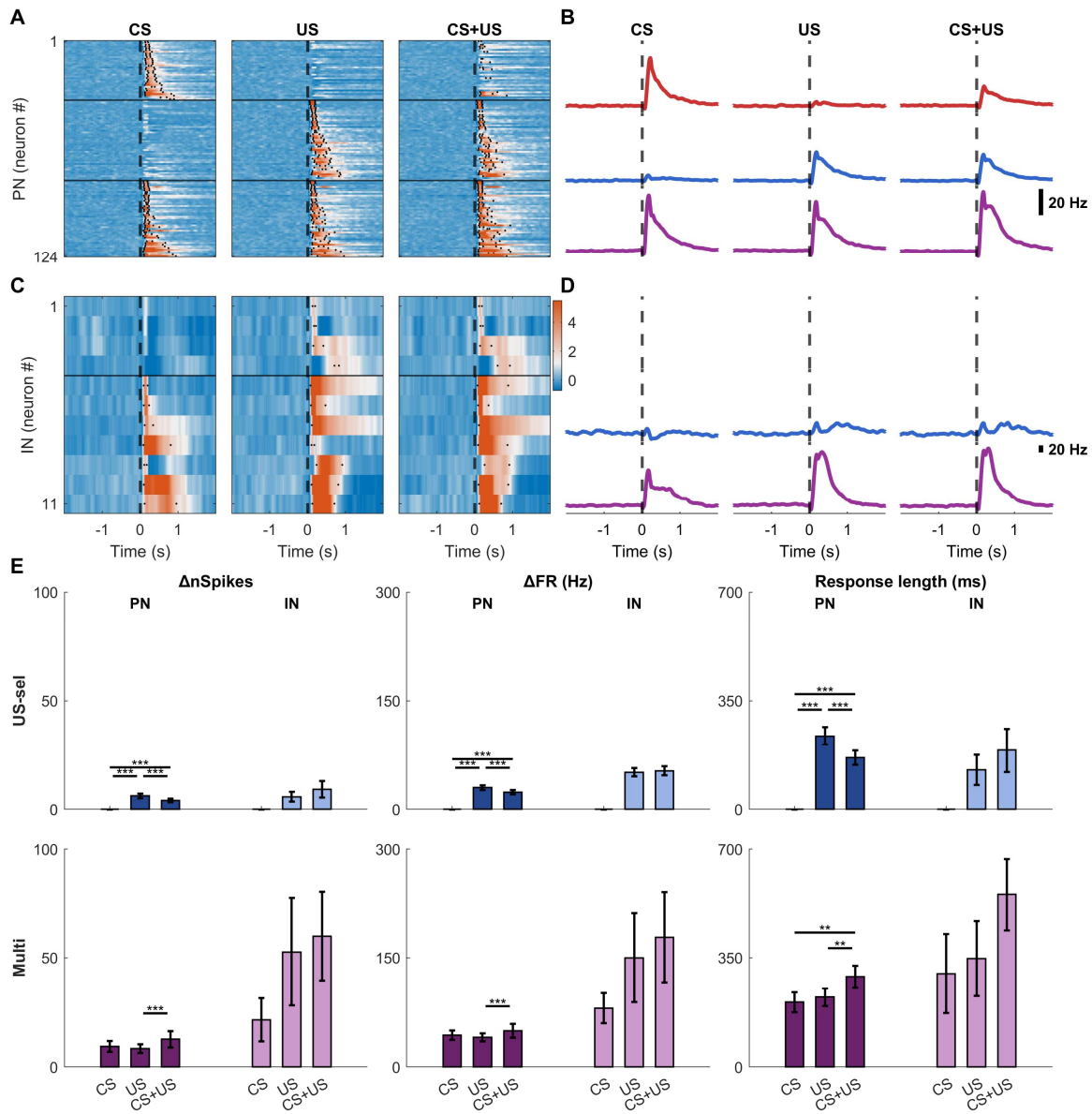
**(A)** Permutation test validating regional differences in cluster distributions. Histogram shows distribution of chi-square statistics from 10,000 permutations (gray bars) with observed chi-square value (red line). P-value indicates probability of observing the actual distribution under the null hypothesis of no regional differences. **(B)** Contingency table showing observed neuron counts for each cluster type across brain regions. Rows represent regions (LA, BA, AStria, CeA), columns represent cluster categories (CS-selective, US-selective, Multisensory, Non-responsive, Inhibited). Title displays observed chi-square statistic. **(C)** Cramér's V effect size matrix quantifying strength of association between regional cluster distributions. Color intensity indicates effect size magnitude (0 to 0.5 scale). Text shows Cramér's V values with significance markers from FDR-corrected pairwise comparisons (\*\* $p<0.001$ , \*\* $p<0.01$ , \* $p<0.05$ ). Diagonal elements not applicable (same region comparison). **(D)** Kruskal-Wallis test results for US-evoked response metrics across LA, BA, and AStria. Two panels show overall Kruskal-Wallis p-values and post-hoc pairwise Mann-Whitney U test results for  $\Delta$ FR (Hz) and response length (ms). Significance markers: \*\*\* $p<0.001$ , \*\* $p<0.01$ , \* $p<0.05$ , ns=not significant.



**Supplementary Figure 3: Statistical analysis of regional cluster distributions and response metrics.**

**(A)** Permutation test validating regional differences in cluster distributions between the LA and AStria. Histogram shows distribution of chi-square statistics from 10,000 permutations (grey bars) with observed chi-square value (red line). P-value indicates

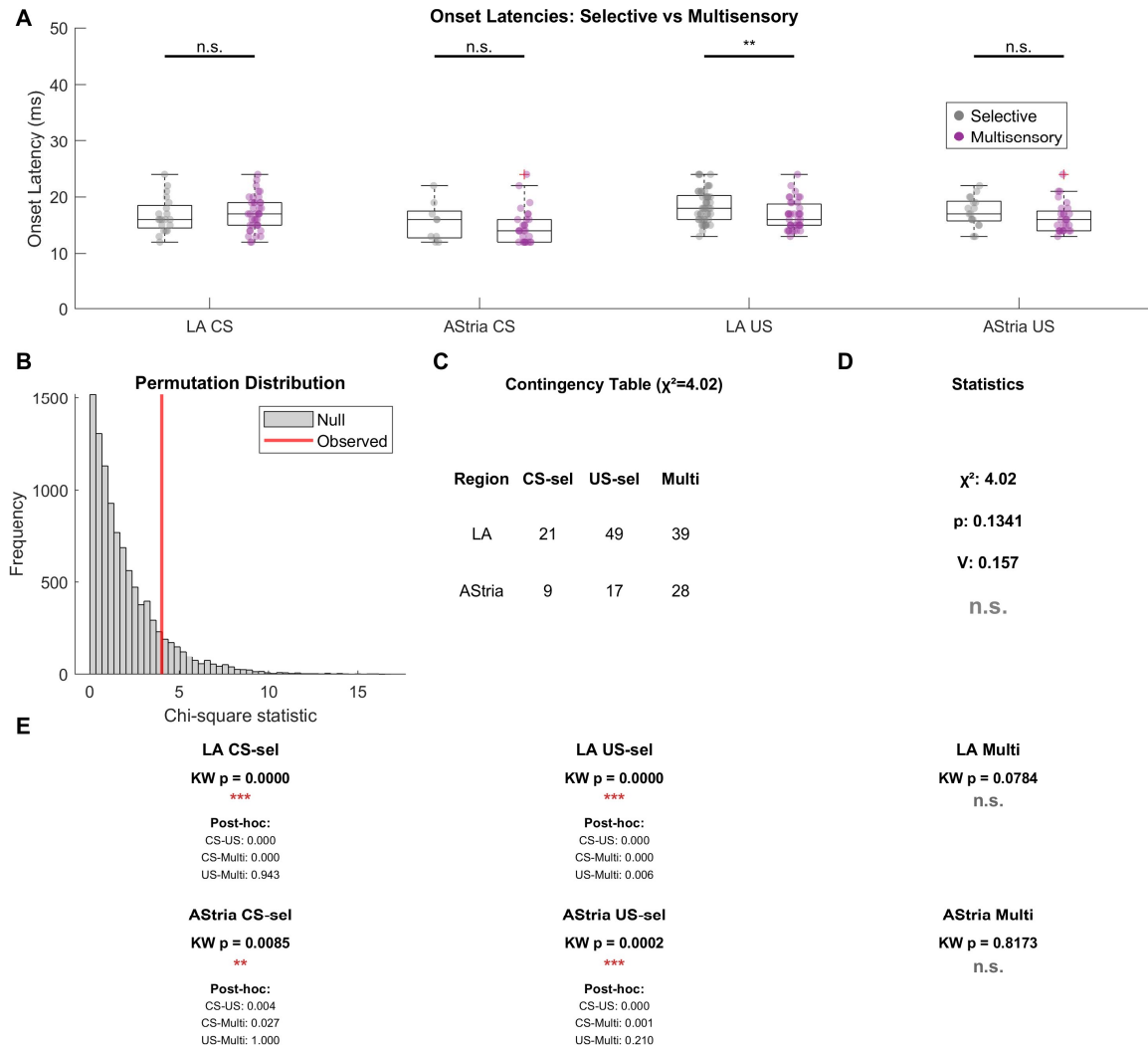
probability of observing the actual distribution under the null hypothesis of no regional differences. **(B)** Contingency table showing observed neuron counts for each cluster type (CS-selective, US-selective, CS+US) in LA and AStria regions. Title displays observed chi-square statistic. **(C)** Statistical summary showing chi-square statistic, permutation p-value, Cramér's V effect size, and significance level (\*\*p<0.001, \*\*p<0.01, \*p<0.05, n.s.=not significant). **(D)** Response metrics comparing CS, US, and CS+US stimuli for CS-selective (row 1), US-selective (row 2), and Multisensory (row 3) neurons. Three columns show  $\Delta$ FR (left, Hz) and response length (right, ms). Darker bars = LA, lighter bars = AStria. Within-region comparisons use Wilcoxon signed-rank test (\*p<0.05, \*\*p<0.01, \*\*\*p<0.001). Significance brackets positioned at two levels with fixed spacing. LA and AStria labels shown in top row. **(E)** Kruskal-Wallis tests comparing CS vs US vs CS+US stimuli within each cluster for each region (6 panels total). Row 5: LA CS-selective, LA US-selective, LA Multisensory. Row 6: AStria CS-selective, AStria US-selective, AStria Multisensory. Each panel shows Kruskal-Wallis p-value with significance level (\*p<0.05, \*\*p<0.01, \*\*\*p<0.001, n.s.=not significant) and post-hoc pairwise Wilcoxon signed-rank test results (CS-US, CS-Both, US-Both). Tests performed on  $\Delta$ FR (Hz) metric.



**Supplementary Figure 4 - PN vs IN: Cell type comparison of response profiles in the lateral amygdala.**

(A) PN (principal neuron) heatmaps showing z-scored PSTHs for CS (left), US (middle), and CS+US (right) stimuli in the LA. Neurons sorted by cluster (CS-selective, US-selective, Multisensory, non-responsive, inhibited) based on CS and US responses only. Color scale shows z-score normalized to baseline. Black lines separate clusters. (B) Lines showing population average firing rates (Hz) for CS-selective (red), US-selective (blue), and Multisensory (purple) neurons. Each cluster displayed separately (stacked rows) for CS, US, and CS+US stimuli. Scale bar: 20 Hz. (C) IN (interneuron) heatmaps, same format as panel A. (D) Lines, same format as panel B. (E) Response metrics comparing PN vs IN for each cluster across three stimuli. Six bar chart panels arranged as 2 rows (PN top, IN bottom)  $\times$  3 columns (CS-selective left, US-selective middle, Multisensory right).

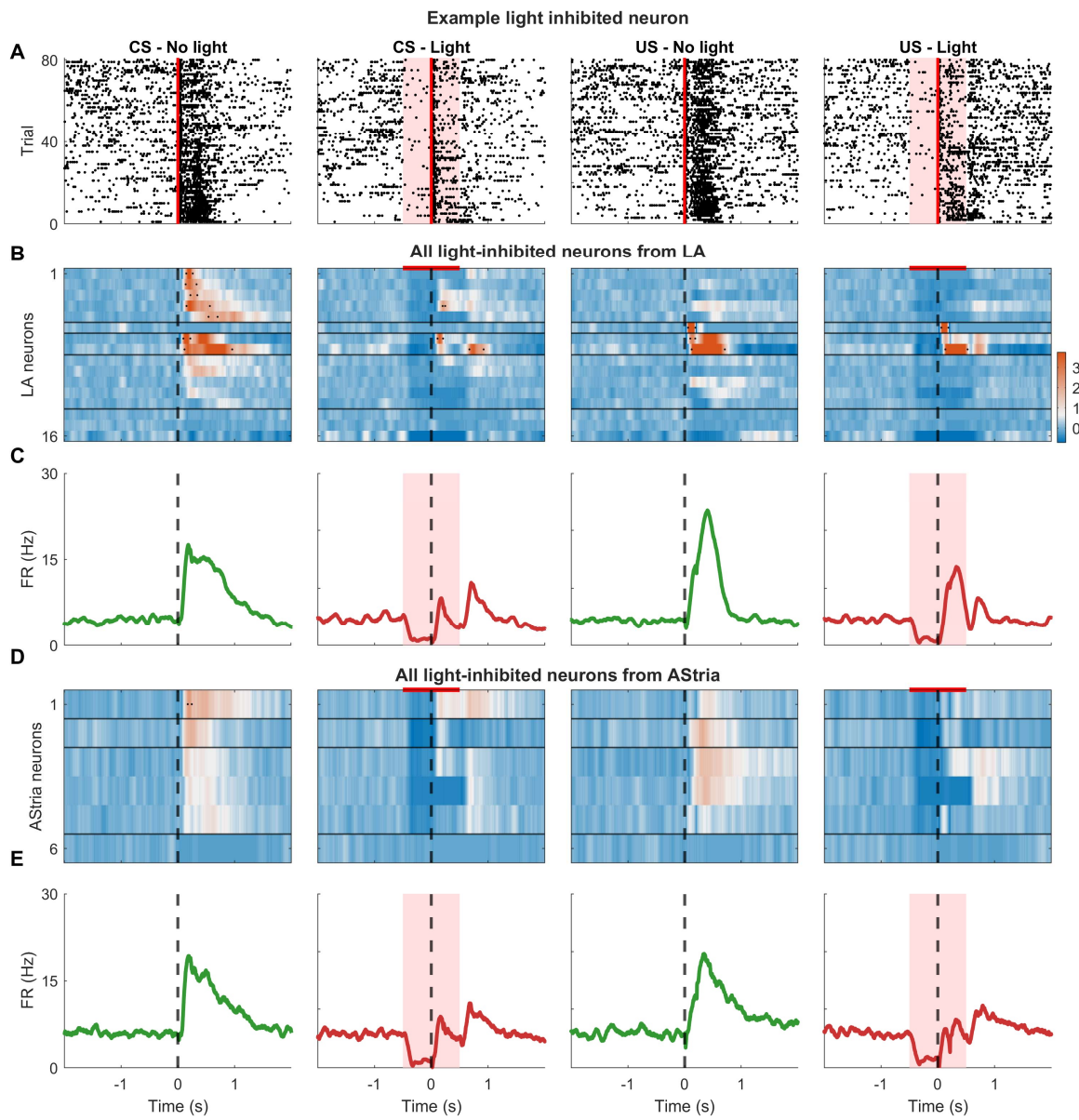
Multisensory right). Each panel shows delta firing rate ( $\Delta$ FR) for CS, US, and CS+US stimuli. Bars show mean  $\pm$  SEM. Statistical comparisons use Wilcoxon signed-rank test (\* $p<0.05$ , \*\* $p<0.01$ , \*\*\* $p<0.001$ ). Color coding matches cluster assignments (red = CS-selective, blue = US-selective, purple = Multisensory).



### Supplementary Figure 5: Monosynaptic onset latency analysis and statistical comparisons

**(A)** Onset latency comparison between selective (CS-selective or US-selective) and Multisensory neurons. Boxplots showing LA CS-selective vs Multisensory (CS latency), LA US-selective vs Multisensory (US latency), LA Multisensory CS vs US latency, AStria CS-selective vs Multisensory (CS latency), AStria US-selective vs Multisensory (US latency), AStria Multisensory CS vs US latency. Median (center line), interquartile range (box), and full data range (whiskers). Statistical comparisons use Wilcoxon rank-sum test (\*p<0.05, \*\*p<0.01, \*\*\*p<0.001, n.s.=not significant). **(B)** Permutation test validating regional differences in monosynaptic cluster distributions between the LA and AStria. Histogram shows distribution of chi-square statistics from 10,000 permutations (grey bars) with observed chi-square value (red line). P-value indicates probability of observing the actual distribution under the null hypothesis of no regional differences. **(C)**

Contingency table showing observed monosynaptic neuron counts for each cluster type (CS-selective, US-selective, Multisensory) in LA and AStria regions. **(D)** Statistical summary showing chi-square statistic, permutation p-value, Cramér's V effect size, and significance level (\*\*p<0.001, \*\*p<0.01, \*p<0.05, n.s.=not significant). **(E)** Kruskal-Wallis tests comparing CS vs US vs CS+US stimuli within each cluster for each region (6 panels total). Row 1: LA CS-selective, LA US-selective, LA Multisensory. Row 2: AStria CS-selective, AStria US-selective, AStria Multisensory. Each panel shows Kruskal-Wallis p-value with significance level (\*p<0.05, \*\*p<0.01, \*\*\*p<0.001, n.s.=not significant) and post-hoc pairwise Wilcoxon signed-rank test results (CS-US, CS-Multi, US-Multi). Tests performed on monosynaptic ΔFR (Hz) metric from bar charts in main figure.



**Supplementary Figure 6: Light-inhibited PV interneurons during optogenetic manipulation.**

**(A)** Example raster plots from a single light-inhibited neuron recorded in PV-Cre mice injected with AAV5-CAG-FLEX-ArchT-tdTomato showing responses to CS and US stimuli. Four columns show CS no-light, CS light, US no-light, and US light conditions. Each row represents one trial with spike times shown as vertical marks. Red vertical line indicates stimulus onset. **(B)** Heatmaps of LA PV interneurons showing z-scored PSTHs for all light-inhibited neurons sorted by stimulus preference. Four panels show CS no-light, CS light, US no-light, and US light conditions. Color scale shows z-score normalized to baseline. PV interneurons sorted to maximize similarity in response

patterns. **(C)** Lines shown average firing rate for light-inhibited neurons. Four panels show mean firing rate (Hz) over time for CS no-light (black), CS light (red), US no-light (black), and US light (red) conditions. Time axis centered at stimulus onset (0 ms). Shaded areas represent SEM. **(D)** Heatmaps of AStria PV interneurons showing z-scored PSTHs for all light-inhibited neurons, same format as panel B. **(E)** Lines show average firing rate for light-inhibited PV interneurons, same format as panel C. Light-inhibited neurons identified using Wilcoxon rank sum test comparing recent baseline (-0.5 to 0s) vs earlier baseline (-5 to -0.5s) with criterion of  $p < 0.05$  and  $\geq 50\%$  firing rate drop.